Pakistan J. Zool., pp 1-10, 2024. **DOI**: https://dx.doi.org/10.17582/journal.pjz/20230207150234

Genotoxicity and Anti-Cancer Activity of Tamoxifen and Ivermectin Loaded Chitosan Nanoparticles Against MCF-7 Cell Line

Usama Bin Naeem[1], Muhammad Adil Rasheed[1]*, Muhammad Ashraf[1] and Muhammad Yasir Zahoor[2]

[1]*Department of Pharmacology and Toxicology, Faculty of Biosciences, University of Veterinary and Animal Sciences, Lahore, Pakistan*
[2]*Institue of Biochemistry and Biotechnology, Faculty of Biosciences, University of Veterinary and Animal Sciences, Lahore, Pakistan*

Article Information
Received 07 February 2023
Revised 22 November 2023
Accepted 08 December 2023
Available online 29 April 2024
(early access)

Authors' Contribution
MAR and MA designed the experiments. UBN carried out the experiments. MAR and MYZ analyzed the data and organized the figures. UBN wrote the manuscript. MAR reviewed the manuscript.

Key words
Tamoxifen, Ivermectin, Genotoxicity, Nanoparticles, Cancer

ABSTRACT

The purpose of this work was to examine the anti-proliferative activity of tamoxifen (TAM) and ivermectin (IVM) loaded chitosan (Cs) nanoparticles against breast cancer cell line (MCF-7) to improve drug delivery to the target sites. Characterization of NPs were carried out by Fourier transform infrared spectroscopy, zeta sizer, potential, morphology by scanning electron microscope, drug entrapment efficiency and *in vitro* drug release. In TAM and IVM loaded chitosan nanoparticles the peaks were at 1606 cm^{-1} and 1640 cm^{-1} respectively. TAM and IVM-CsNPs have size 189 and 196 nm with positive charge. The morphology of both nanoparticles were spherical and smooth surface. Drug entrapment efficiency was 79.08 ± 1.3 % and 89.00 ± 0.043 % respectively. At pH 6.0 and 7.4, drug released from Cs-NPs in biphasic manner, with an initial burst occurring during first 6–12 h and a steady release lasting for 48 h. Inhibitory concentration value of free drugs and nanoparticles alone and in combination with selectivity index (SI) were calculated that was > 2. SI of drugs and CsNPs are > 2 which showed cytotoxicity towards cancerous cells. Genotoxicity assessment showed slight damage by TAM and IVM to the mean tail length of DNA as compared to nanoparticles. These results suggest that TAM and IVM loaded CsNPs may be promising alternative to current treatment against breast cancer.

INTRODUCTION

Breast cancer affects around one in five cancer patients worldwide. Breast cancer is the main reason why women die from cancer. There are several different chemotherapy medications used to treat breast cancer (Malik *et al*., 2012). Systemic toxicity and unfavorable effects result from the anticancer medications' inability to distinguish between malignant and normal cells. As a result, the maximum allowed dose of the medication is significantly decreased. Drug penetration into cancer cells from normal formulations is very restricted due to low dispersion and quick clearance. The tissue needs more medication because of the widespread distribution and rapid evacuation from the targeted organs, which leads to unwanted toxicity and is economically unsound (Majir *et al*., 2014).

In order to distribute these chemotherapeutic drugs in a regulated manner, nanoparticles are crucial. Drug delivery by nanoparticles enables the achievement of targeted drug concentration at specified site, limiting side effects and toxicity, dose dumping, etc. (Divya and Jisha, 2018). Three functional group in addition to main and secondary hydroxyl groups at the C2, C3, and C6 positions, chitosan also contains an amino group. Chitosan's reactive hydroxyl groups undergo a chemical shift by being attached to side groups, but its biophysical qualities are unaffected (Abdel-Aziz *et al*., 2016).

Tamoxifen (TAM) is a potent hydrophobic endocrine drug, is typically used to treat breast cancer and reduce risk in those who are at high risk (Day *et al*., 2020). TAM may have an estrogenic or an antiestrogenic effect, depending on the dosage and the tissues treated. However, TAM therapeutic efficacy is negatively impacted by considerable hepatic metabolism and poor oral bioavailability. Long-term TAM treatment has some undesirable side effects,

* Corresponding author: dr_aadil@uvas.edu.pk
0030-9923/2024/0001-0001 $ 9.00/0

including the development of endometrial cancer, liver cancer, increased blood clotting, ocular retinopathy, and corneal opacity (Moin *et al*., 2021).

Ivermectin (IVM) is produced from avermectin and has a 16-membered ring with 80 % 22, 23-dihydroavermectin-B1a and 20 % 22, 23-dihydroavermectin-B1b. IVM is a macrolide antiparasitic medication. Along with IVM, the avermectin family currently consists of selamectin, doramectin, and moxidectin. In 1978, the FDA approved the use of IVM as an antiparasitic therapy for people (Laing *et al*., 2017). It is currently the avermectin class drug that is most commonly utilized. Gamma-aminobutyric acid (GABA) is released by the parasite when IVM opens glutamate-gated chloride channels, which destroy neurons. This causes a sizable amount of chloride ion inflow, neuronal hyperpolarization, and somatic muscle paralysis to kill parasites (Tang *et al*., 2021). The Akt/mTOR pathway needed to be suppressed in order to induce autophagy as part of the IVM anticancer strategy, and PAK1 was the target for breast cancer (Dou *et al*., 2016). Additionally, Diao's research shows that IVM could arrest the cell cycle in the canine breast cancer cell lines CMT7364 and CIPp without increasing apoptosis, and the IVM mechanism may be connected to the suppression of the Wnt pathway (Diao *et al*., 2019).

In order to improve medication delivery to the target locations, this study looked into the *in vitro* evaluation of chitosan (Cs) loaded nanoparticles of tamoxifen (TAM) and ivermectin (IVM) against breast tumors utilizing the MCF-7 cell line. The aim was to determine the anticancer activity of nanoparticles against breast cancer cell line (MCF-7) using MTT assay and to evaluate the genotoxicity.

MATERIALS AND METHODS

IVM, polyvinyl alcohol (MW 125,000; S.D. Fine Chem. Pvt. Ltd., Mumbai, India), chitosan (MW 50,000–75,000), Dulbecco's Modified Eagle's Medium (DMEM), foetal bovine serum, and the tetrazolium dye were all acquired from Sigma-Aldrich Co. in St. Louis, Missouri. The additional materials were all of the analytical reagent quality.

Preparation and characterization of nanoparticles

Nanoparticles of TAM and IVM were prepared by a technique called ionic gelation. Nanoparticles of both drugs separately obtained upon mixing 45 mg of Cs that was dissolved in 1 % acetic acid solution then 10 mg of IVM and 10 mg of TAM were added in it and continuously stirrer at 200 rpm for 30 min at 25 °C. A solution of tripolyphosphate (1 mg ml^{-1}) was dissolved in distilled water and added drop wise in the solution. The mixtures were stirred at 600 rpm for 30 min at room temperature using a magnetic stirrer. By adding a 1 M solution of NaOH, the pH was changed (4.8–5.5). After that, each drug's nanoparticles were removed from the solution by centrifuging (18,000 rpm) for 45 min at 10 °C. The supernatant was used to evaluate the encapsulation rate and the resulting sediment was freeze dried and used for further studies (Nokhodi *et al*., 2022).

NPs were characterized by Fourier transform infrared spectroscopy (FTIR), zeta sizer, zeta potential, morphology study by scanning electron microscope (SEM), drug entrapment efficiency and *in vitro* drug release.

FTIR

Using an FTIR 8300 spectrophotometer, the FTIR of Cs, TAM nanoparticles, and IVM were obtained (Shimadzu, Japan). Each sample was blended with dry KBr and 2 % (w/w) KBr disc. The mixes were compressed into KBr discs for 30 sec while being subjected to a hydraulic pressure of 10,000 psi. An agate mortar was used to crush the mixtures into a fine powder. Each KBr disc was scanned at a speed of 4 mm/s with a resolution of 2 cm^{-1} over a wave number range of 4,000-400 cm. Different samples' characteristic peaks were recorded.

Determination of particle size and zeta potential

Using a dynamic light scattering approach at 25 °C, the Zeta sizer nano ZS90 (Malvern Instruments, Malvern, UK) was used to measure the average particle sizes, polydispersity indices, and zeta potentials of nanoparticles. Samples were diluted with Milli-Q (Millipore Corp.) water before testing.

SEM

The external morphology of nanoparticles was examined using SEM (Model-JSM-6700F; JEOL, Tokyo, Japan). The samples were coated with platinum at a 5 kV acceleration voltage prior to observation.

Determination of drug entrapment efficiency

It was indirectly established how much of the medications TAM and IVM were integrated into nanoparticles. Following the ultracentrifugation of nanoparticles, the supernatant of both medications including free drug was diluted in methanol, and the samples were analyzed spectrophotometrically at wavelengths of 260 nm and 236 nm, respectively (Jasco V630 BIO). The following equation was used to obtain the encapsulation efficiency (EE) in triplicate (Altmeyer *et al*., 2016).

$$\% EE = A_{initial} - A_{free} / A_{initial} \times 100$$

In vitro *drug release study*

The release behaviour of TAM and IVM from nanoparticles was investigated at pH 4.0 (about the pH in endosomes or lysosomes), pH 6.0 (the environment around the tumors), and pH 7.4. (pH of physiological blood). TAM and IVM loaded chitosan nanoparticles were placed in a dialysis bag (Spectra/Por®; Spectrum Laboratories, Inc., Rancho Dominguez, CA) and then dissolved in PBS (pH 7.4) for five milliliters. The dialysis bag was then filled with 95 mL of PBS with a pH of 5.0, 6.0, or 7.4. The release media was continuously agitated with a stirrer at 50 g and 37 °C. At predetermined intervals, 2 mL of the external medium were removed and swapped out for identical, brand-new PBS. At 254 nm, the amount of released TAM and IVM in the media was measured using a spectrophotometer (Vivek *et al*., 2013).

In vitro *anticancer activity*

At 37 °C, the cells were grown in DMEM media, which is Dulbecco's modified Eagle's medium with 10 % fetal bovine serum, 1% penicillin, and streptomycin added as supplements. The *in vitro* anticancer activity was evaluated using the MTT test (Moin *et al*., 2021). 96-well plates with Vero and MCF-7 cells each were planted for 24 h. The cells were then cultivated for a further period of time at 37 °C in an incubator with 5 % CO_2, after which the culture medium was discarded and fresh medium containing progressively higher concentrations (25-400 µg/ml) was added. After 72 h had passed since the start of the incubation period, MTT reagent (0.5 mg/ml) was added to each well, and cells were then incubated at 37 degrees Celsius for 4 h. Then, to dissolve formazan crystals, DMSO solution was added to each well. The absorbance of each well was taken at 570 nm using an ELISA reader (ELX-800 Biotek, Winooski, VT). For each condition, the data are shown as the mean and standard deviation (SD) of three samples. Drugs were used alone and in combination against both the cell lines (TAM, IVM, TAM-CsNPs, IVM-CsNPs, TAM + IVM, TAM-CsNPs + IVM, IVM-CsNPs +TAM).

The viability, cell survival and selectivity index were calculated as follows.

$$\%\ \text{Viable cells} = \frac{\text{Number of viable cells/ml}}{\text{Total number of cells/ml}} \times 100$$

$$\text{Cell survival} = \frac{\text{Mean OD of test} - \text{Mean OD of negative control}}{\text{Mean OD of positive} - \text{Mean OD of negative}} \times 100$$

$$\text{Selectivity index} = \frac{\text{IC50 of pure compound in a normal cell line}}{\text{IC50 of pure compound in cancerous cell line}}$$

Genotoxicity

Genotoxicity was assessed by single-cell gel electrophoresis (COMET assay). The extracted lymphocytes were exposed to different concentrations of drugs and nanoparticles alone and in combination. After being treated with trypsin to obtain a single cell solution, 1.5×10^4 cells were immediately pipetted onto a cavity grove slide that had been precoated before being embedded in 0.75% low melting agarose. Samples were lysed after 4 h at 50 °C in EDTA with a pH of 8.0. Materials were electrophoresed for 25 min at 0.6 v/cm and stained with ethidium bromide after being in Tris/borate/EDTA buffer with a pH of 8.0 overnight. A charge-coupled device fluorescence microscope was used to analyse the slides, and comet photographs from each sample were studied for the tail moment, DNA content, and tail percentage DNA (Abdellatif *et al*., 2022). Dimethyl sulfoxide (DMSO) was used for both positive (20%) and negative (1%) control. Each cell was divided into four groups according to their tail length (Dhawan *et al*., 2009).

Statistical analysis

The data was calculated as mean (±) standard deviation, and statistically significant differences will be assessed using one-way Analysis of Variance (ANOVA) with p-values of < 0.05 in the statistical package for social sciences.

RESULTS AND DISCUSSION

Characterization of prepared nanoparticles

FTIR spectroscopy was used to examine how the medication and polymer interacted (Fig. 1). The free tamoxifen's FTIR spectra revealed bands at 1247 cm^{-1} of quaternary ammonium by N-H stretching, 1600 cm^{-1} of aromatic C-C, 726 cm^{-1} of monosubstituted aromatic benzene, 1746 cm^{-1} of citrate's carbonyl band, and 3422 cm^{-1} of its 10 hydroxyl. TAM-loaded chitosan nanoparticles show three peaks at 2992 cm^{-1} (OH), 1606 cm^{-1} (C-O-C), and 1083 cm^{-1} (NH). In contrast, the peak 3422 cm^{-1} of the Cs nanoparticles loaded with TAM was much wider than TAM, demonstrating hydrogen bond stretching. TAM-loaded chitosan nanoparticles were found to have moved a peak at 1606 cm^{-1} that had been observed in the drug. While another investigation revealed that TAM-loaded PLGA nanoparticles and other polymers with IR stretching vibration zone functional groups showed peaks at 1300 cm^{-1} and 1200 cm^{-1}, including PLGA, polyvinyl acetate (PVA), and PLGA (C-O and C-N) (Mukherjee *et al*., 2008) While van der Waals forces or dipole-dipole interactions between (C-N) in the drug and (-OH) in PLGA and PVA were present, these interactions led to the formation of weak physical bonds like hydrogen (Sahana *et al*., 2010).

Cs nanoparticles with IVM loaded showed an absorption band at 1267 cm^{-1} (N-H) of the amide and ether linkages. The secondary hydroxyl group peaks, which

were observed at 1032 cm^{-1} and 1423 cm^{-1}, respectively, were at 3465 and 2902 cm^{-1}. The nanoparticle peak for both Cs and IVM is 1640 cm^{-1}. The FTIR spectra of IVM showed the distinctive prominent peaks in the range 700-1250 cm^{-1}. In contrast to IVM-SLNs and IVM alone, wave number at 3483 cm^{-1} depicted (O-H) stretching, and a sharp absorption band that was visible around 2935 cm^{-1} corresponded to (C-H) stretching. In IVM-SLNs, however, a stretching band of the C6-ring stretching could be attributed to wave number at 1732-703 cm^{-1} (Guo *et al.*, 2018).

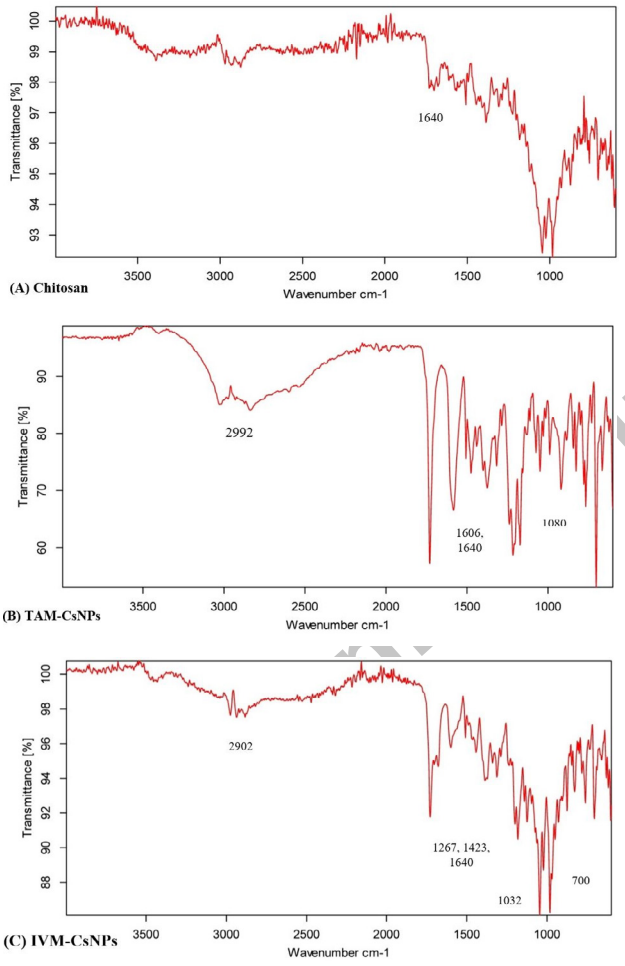

Fig. 1. Fourier transform infrared (FTIR) spectroscopy. (A) Chitosan; (B) TAM-CsNPs; (C) IVM-CsNPs.

Particles size and charge of TAM and IVM nanoparticles are shown in Figure 2. Average size of the TAM was 189 nm and IVM was 196 nm with polydispersity index is 0.367 and 0.350, respectively. The zeta potential showed values between +24.3 and +28.1 mV, showing that value was dropping as drug concentration increased. Other tests showed that the PDI value of the tamoxifen-loaded silk fibroin nanoparticles (TC-SF-NPs) was 0.169 ± 0.01 and indicated a homogeneous size distribution (Abdallah *et al.*, 2021). While the equivalent size distribution in IVM-SLNs is shown as a histogram with a mean diameter of 270.34 nm and a range of 150 to 400 nm with a PDI value of 0.082 (Mitri *et al.*, 2011). Because of the strong positive charge of the Cs polymer, IVM-loaded CS-ALG nanoparticles had a positive zeta potential (+36.23) (Ali *et al.*, 2013).

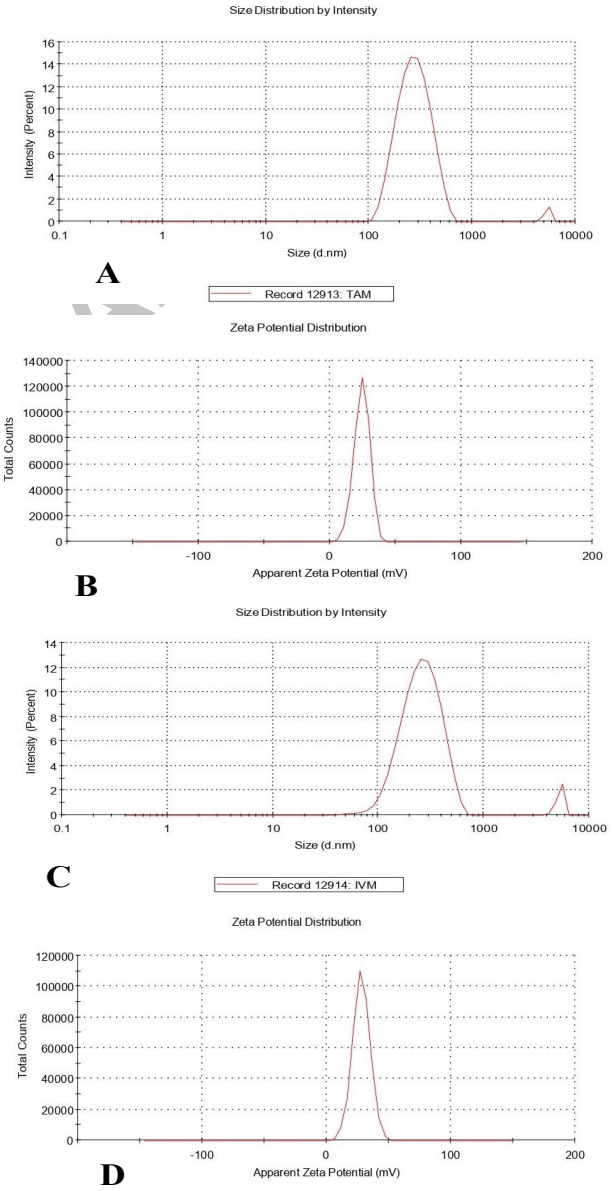

Fig. 2. Zeta sizer and zeta potential of TAM-CsNPs and IVM-CsNPs. (A) TAM-CsNPs; (B) TAM-CsNPs; (C) IVM-CsNPs; (D) IVM-CsNPs.

When compared to PLGA-loaded TAM nanoparticles, the charge of different batches ranges from -10.5 mV to -16.5 mV. The charge of TAM-CsNPs was +24.3 mV and IVM-CsNPs was +28.1 mV. The zeta potential can be used to explain the electrostatic potential at a particle's surface. An absolute charge range of -30 mV to +30 mV indicates that the particles are less likely to aggregate quickly in a liquid state and would likely remain suspended for a longer period of time (Basu *et al*., 2012). Larger values of charge, whether positive or negative, tend to stabilize the suspension and lessen the possibility of aggregation for charged particles. The charge on IVM-SLNs was 30.5 ± 1.51 mV, which indicated that the particles would be stable over the long term (Meibner *et al*., 2009).

The prepared nanoparticles of IVM and TAM had smooth surfaces and were spherical in shape (Fig. 3). The tamoxifen TC-SF-NPs demonstrated that nanoparticles were round and circular with dense cores, in contrast to other formulations (Ghanbarzadeh *et al*., 2015), IVM-SLNs, however, were quite homogeneous in shape and had an almost spherical shape (Honary *et al*., 2013) and IVM-loaded NLC suggests that the solution's polymeric nanoparticles were evenly dispersed (Ahmadpour *et al*., 2019).

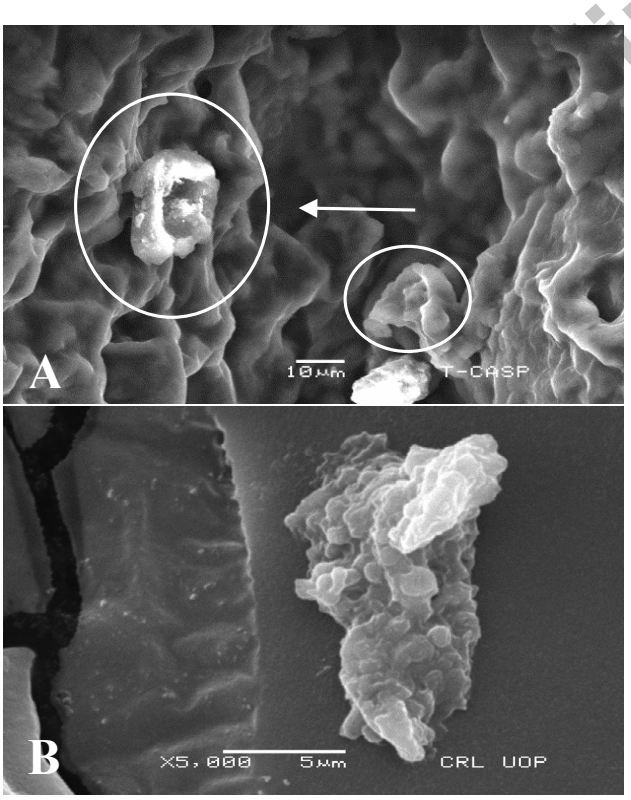

Fig. 3. Scanning electron microscope (SEM). (A) TAM-CsNPs; (B) IVM-CsNPs.

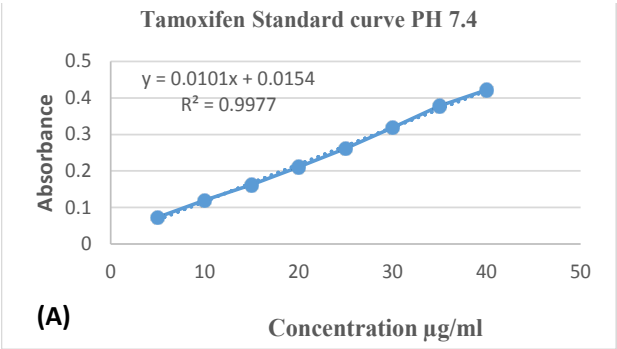

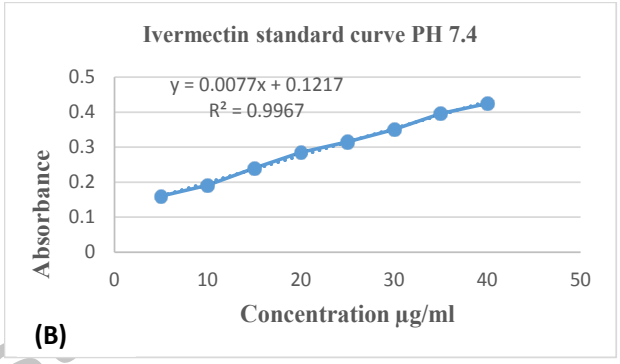

Fig. 4. Drug entrapment efficiency of (A) TAM-CsNPs (B) IVM-CsNPs at pH 7.4.

Determination of drug entrapment efficiency

In this standard curve absorbance of particles were represented by Y. Whereas, R^2 indicated the association factor the standard calibration curve of TAM and IVM shown in Figure 4, respectively where the dotted line represented the experimental data and the constant line represented the regression equation: y = 0.0101x - 0.0154 R^2 = 0.9977 and y = 0.0077x - 0.1217 R^2 = 0.1217 of TAM and IVM. With the help of standard calibration, the percentage entrapment of chitosan loaded IVM and TAM nanoparticles were 79.08 ± 1.3 % and 89 ± 0.043 %, respectively. Another study found that ristearin solid lipid nanoparticles (TSSLN) had the lowest entrapment efficiency (78.78%) compared to tripalmitin solid lipid nanoparticles (TPSLN) and glycerol behenate solid lipid nanoparticles (GBSLN) (98.64%). The presence of mono and diglycerides contributes to GBSLN's higher entrapment efficiency when compared to other lipids (Harivardhan *et al*., 2006). While TC was effectively trapped within SF-NPs with entrapment efficiencies of 38.29 ± 0.63 % and 79.08±1.2 %, respectively (Moin *et al*., 2021). Previously study reported that the drug EE of the IVM-SLNs formulation was 98.48 ± 0.052% (Laing *et al*., 2017). In comparison to IVM-CsNPs, PLGA-loaded IVM formulations (F1–F6) had values ranging from 79 ±

0.729 to 234 ± 0.784 and 70.49 ± 0.983 to 80.307 ± 0.354, respectively. IVM's high entrapment efficiency (74.12 %) was a result of the drug's better solubility in the solvent utilized (Ali *et al*., 2014).

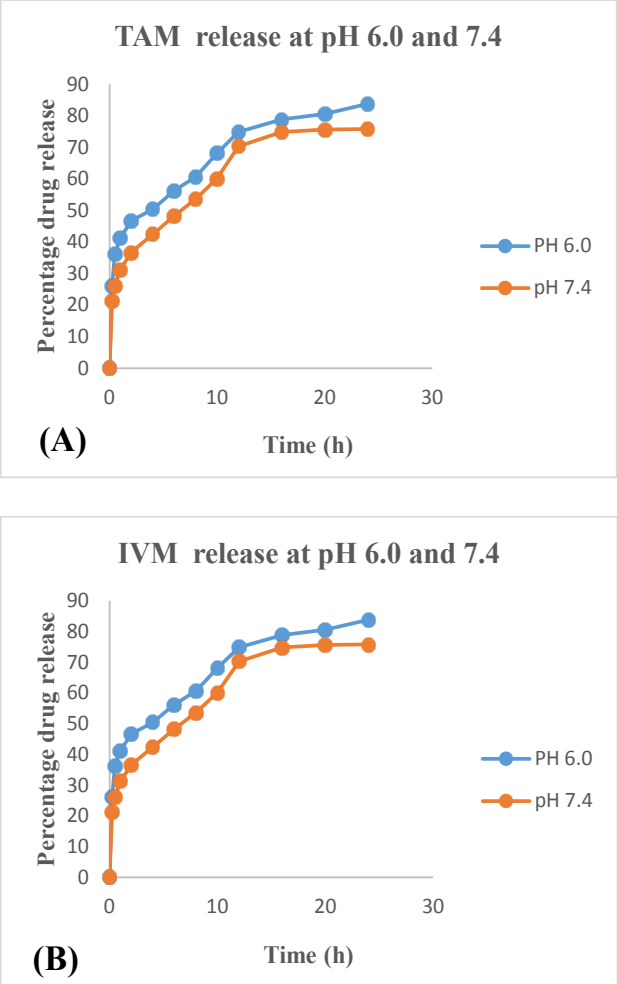

Fig. 5. *In vitro* drug release of TAM-CsNPs (A) and IVM-CsNPs (B) at 6.0 and 7.4 pH for 24 h.

In vitro *drug release*

At pH 7.4 and pH 6.0, respectively, *in vitro* release of chitosan-loaded IVM and TAM nanoparticles was investigated. Both pH levels showed a burst release from IVM nanoparticles, with 31.48±75.82 % and 47.48±83.8 % of the drug released over the course of 24 h at pH 7.4 and pH 6, respectively. For TAM, 24.18±58.51 % and 29.41±65.21 % of the drug released over the course of 24 h at pH 7.4 and pH 6, respectively (Fig. 5). On another hand, the higher drug entrapment efficiency, which may cause faster drug release, and on the other, the recognition and the initial burst of drug release from nanoparticles may result from the rapid release of drug molecules that are situated near the hydrophobic-hydrophilic line of the nanoparticles. According to a study, chitosan-loaded tamoxifen released slowly and consistently at pH 7.4, with a 24 h release ratio of around 22 ± 0.21 %. Tamoxifen discharged between 43 ± 0.45 % of its total amount (pH 6.0) and 68 ± 0.34 % (pH 4.0) in a 24 h period when the pH was lower. Lower pH levels caused the medication to protonate, releasing drug molecules into the medium (Zahangh *et al.,* 2012) while, Tripalmitin solid lipid nanoparticles (TPSLN), glycerol sulphate solid lipid nanoparticles (GSSLN), and TSSLN were shown to have t_{25} values of 5, 6.5, and 8.7 h, respectively, for 25 % drug release. In comparison to solid lipid nanoparticles, the t50 (time taken for 50 % drug release) values were found to be 13.2, 19 and 38.5 h, respectively (Harivardhan *et al*., 2006). IVM-PLGA in PBS (pH 7.4) demonstrated an early burst release of around 20.80 % in the first 30 min, followed by a progressive sustained release phase of approximately 98.29 % up to 24 h, according to another study (Ali *et al*., 2014).

Table I. IC_{50} and selectivity index of Tamoxifen (TAM) and Ivermectin (IVM) NPs alone and in combination.

Drugs	IC_{50} µg/ml		Selectivity index
	Vero	MCF-7	
Tamoxifen	56.8	8.02	7.08
Ivermectin	93.24	18.56	5.02
TAM + IVM	69.87	11.09	8.73
TAM-CsNPs	47.33	5.86	8.07
IVM-CsNPs	54.87	9.14	6.0
TAM-CsNPs + IVM	48.05	8.0	6.0
IVM-CsNPs +TAM	50.45	9.16	5.38

This table shows the activity of Drugs and Nanoparticles alone and in combination on two different cell lines to evaluate the anti-cancer activity. TAM, Tamoxifen; IVM, Ivermectin.

Anticancer activity

Anticancer activity by MTT assay was performed on cancerous cells line (MCF-7) and non-cancerous cell line (Vero). The results demonstrated that IVM and TAM were effective to reduce the viable cells at high concentrations (125, 62.5, 31.25 and 15.62 µg/ml), while on the other hand IVM-NPs and TAM-NPs showed effect at concentrations (62.5, 31.25, 15.62 and 7.8 µg/ml), respectively. In combination study the drugs and nanoparticles were demonstrated the anticancer activity at lower doses (15.62, 7.8 and 3.0 µg/ml) with selectivity index 5.38, 6.0 and 8.73, respectively. The IC_{50} value of free drugs and nanoparticles alone and in combination of free drugs with nanoparticles were shown Table I. Compared to alternative formulations TC had IC_{50} values of 56.49 and 86.83 mg/ml against MCF-7 and MDA-MB-231 cells, respectively, while TC

loaded SF-NPs had IC_{50} values of 86.91 and 107.17 mg/ml against the same two cell types (Moin *et al*., 2021). The IC_{50} value of the produced NPs in another investigation using tamoxifen-loaded magnetic iron oxide coated with L-lysine nanoparticles was 11.3 µg/ml after 24 h, demonstrating that the concentration of IC_{50} reduced with longer treatment times. The predicted IC_{50} levels for TAM in MCF-7 were 4.4 µg/ml for 24 h, respectively. The MTT assay revealed that the cytotoxicity of F-Lys NPs on MCF-7 cells was extremely low. After 24 h, the F-Lys NPs' IC_{50} concentrations in MCF-7 cancer cells were 563.37 µg/ml, respectively (Rostami *et al*., 2022). In IVM the IC50 values on ovarian cancer were 29.46 µg/ml for IOSE80 cells, 20.85 µg/ml for SKOV3, and 22.54 µg/ml for TOV-21G (Zhan *et al*., 2021). Ivermectin was applied to six breast cancer cell lines for 24 h (MCF-7, MDA-MB-231, MDA-MB-468, MDA-MB-361, MDA-MB-435, and HS578T) as well as a non-tumorigenic human breast cell line (MCF-10A), and the IC_{50} value in MCF-10A cells was much greater than that in breast cancer cells. These results demonstrate that ivermectin inhibits the *in vitro* proliferation of breast cancer cells (Dou *et al*., 2016). Lower clonogenic survival consistently indicated that ivermectin severely reduced cell proliferation in MCF-7 and MDA-MB-231 cells.

Genotoxicity assessment

By using 20% DMSO as a positive control and 1% DMSO as a negative control, the genotoxic potential of TAM and IVM loaded chitosan nanoparticles was assessed at concentrations of 31.25 µg/ml, 15.62 µg/ml, and 7.815 µg/ml, respectively. Table II and Figure 6 provide the mean head and tail length of DNA damaged by medicines and nanoparticles alone and in combination. The mean tail length at IC_{50} concentration examined was 11.32±0.39 µm, which is roughly half of that obtained for both medicines and nanoparticles at this concentration and was much shorter than the tail length of damaged DNA produced by

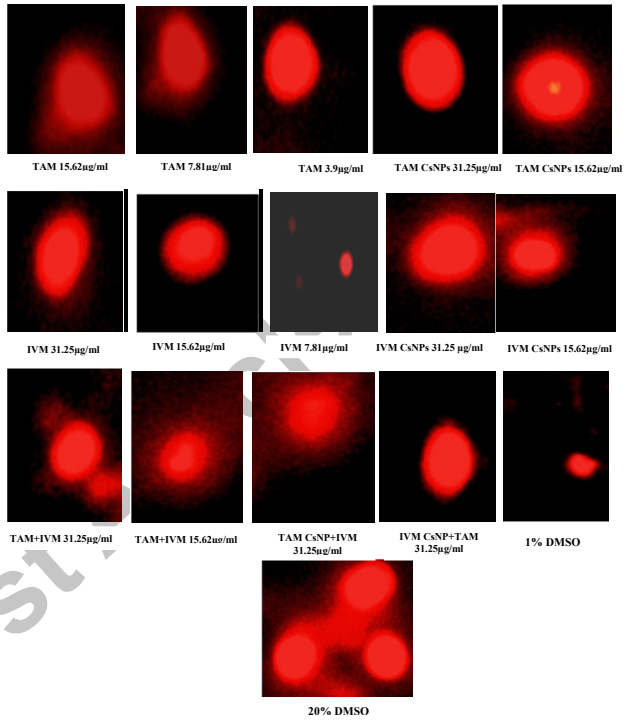

Fig. 6. Comets taken from a fluorescent microscope representing DNA damage since the head size is greater than length of tail (Comet formation).

Table II. Mean head and tail length of damaged DNA for Tamoxifen (TAM) and Ivermectin (IVM) loaded chitosan nanoparticles.

Drugs	Mean DNA head length after different concentrations of drugs (µm) n=25				Mean DNA tail length (µm) after different concentrations of drugs n=25			
	31.25 (µg/ml)	15.62 (µg/ml)	7.815 (µg/ml)	3.9 (µg/ml)	31.25 (µg/ml)	15.62 (µg/ml)	7.815 (µg/ml)	3.9 (µg/ml)
Tamoxifen		2.02±0.63	3.67±0.76	4.46±0.82		1.03±0.28	0.82±0.26	0.22±0.33
Ivermectin	3.48±0.66	4.33±0.62	4.89±0.86		0.77±0.41	0.21±0.32	0.14±0.50	
TAM-CsNPs		3.98±0.85	4.73±0.71	5.43±0.79		0.06±0.11	0.03±0.18	0.12±0.22
IVM-CsNPs		3.22±0.57	3.89±1.02	4.22±0.78		0.16±0.32	0.44±0.83	0.09±0.22
TAM + IVM		1.93±0.45	2.77±0.67	4.54±0.34		1.12±0.31	0.79±0.63	0.34±0.12
TAM-CsNPs + IVM		2.96±0.44	3.06±0.39	3.98±0.11		0.72±0.24	0.29±0.14	0.19±0.34
IVM-CsNPs +TAM		3.09±0.22	3.66±0.13	4.08±0.19		0.62±0.13	0.55±0.19	0.41±0.08
	Positive control				Negative control			
1% DMSO	11.32±0.39				0.12±0.01			
20% DMSO	0.89±0.01				6.25±0.15			

sthe positive control 20% DMSO. One-way ANOVA and post hoc Duncan statistical analysis revealed a highly significant difference ($P<0.05$) between the mean tail lengths at all tested doses and the positive control, indicating that DNA damage to lymphocytes is less at all tested doses than the positive control and similar to the negative. Another study presents numerical values for percentage of DNA in the tail, tail length and tail moment of comets of lymphocytes and MCF-7 cells. In both cell types, TAM induced a significant increase of these parameters at all concentrations except percentage of DNA in the tail and tail moment values for MCF-7 cells treated with TAM at 11 µg/ml However, higher increase of DNA damage in lymphocytes 3.39±0.3 versus 41.79±1.81 than in MCF-7 cells 14.42±2.35 versus 42.19±4.77 (Wozniak *et al*., 2007). Another study stated that ivermectin treated with $CHOK_1$ cells with a concentration ranging 5.0, 25 and 50.0 µg/ml with damage of 3.3±1.2, 0.7±0.3 and 3.0±1.3 a clear increase in IVM-induced DNA damage over control values was revealed as a significant enhancement of the proportion of slightly damaged cells (Molinari *et al*., 2009).

CONCLUSION

The results of this study point to Cs nanoparticles that have been loaded with TAM and IVM as a potentially effective alternative to the standard therapy for breast cancer. Breast cancer cells *in vitro* efficiently absorbed CsNPs, suggesting that they may be used to treat breast cancer. The free medicine was more effective on MCF-7 cells because they preferred to pick up nanoparticles over TAM and IVM. However, with the nanoparticles, *in vivo* research is necessary.

ACKNOWLEDGEMENT

We would like to thank all authors responsible for the insights that we attempted to summarize.

Funding

This work was funded by department of Pharmacology and Toxicology University of Veterinary and Animal Sciences Lahore Pakistan.

IRB approval

There is no need of IRB approval for *in vitro* investigations.

Statement of conflict of interest

The authors have declared no conflict of interest.

REFERENCES

Abdallah, M.H., Lila, A.S., Unissa, R., Elsewedy, H.S., Elghamry, H.A., Soliman, M.S., 2021. Preparation, characterization and evaluation of anti-inflammatory and anti-nociceptive effects of brucine-loaded nanoemulgel. *Colloids Surf. B.,* **205**: 111868. https://doi.org/10.1016/j.colsurfb.2021.111868

Abdel-Aziz, H.M., Hasaneen, M.N. and Omer, A.M.J.S.J.O.A.R., 2016. Nano chitosan-NPK fertilizer enhances the growth and productivity of wheat plants grown in sandy soil. Span. *J. agric. Res.,* **14:** e0902-e0902. https://doi.org/10.5424/sjar/2016141-8205

Abdellatif, A., Ali, A.T., Bouazzaoui, A., Alsharidah, M., Al-Rugaie, O., 2022. Formulation of polymeric nanoparticles loaded sorafenib; evaluation of cytotoxicity, molecular evaluation, and gene expression studies in lung and breast cancer cell lines. *Nanotechnol. Rev.*, **11**: 987-1004. https://doi.org/10.1515/ntrev-2022-0058

Ahmadpour, E., Godrati-Azar, Z., Spotin, A., Norouzi, R., Hamishehkar, H., Nami, S., Heydarian, P., Rajabi, S., Mohammadi, M. and Perez-Cordon, G., 2019. Nanostructured lipid carriers of ivermectin as a novel drug delivery system in hydatidosis. *Parasit. Vectors,* **12:** 1-9. https://doi.org/10.1186/s13071-019-3719-x

Ali, M., Afzal, M., Verma, M., Bhattacharya, S.M., Ahmad, F.J., Samim, M., Abidin, M.Z. and Dinda, A.K., 2014. Therapeutic efficacy of poly (lactic-co-glycolic acid) nanoparticles encapsulated ivermectin (nano-ivermectin) against brugian filariasis in experimental rodent model. *Parasitol. Res.,* **113:** 681-691. https://doi.org/10.1007/s00436-013-3696-5

Ali, M., Afzal, M., Verma, M., Misra-Bhattacharya, S., Ahmad, F.J. and Dinda, A.K., 2013. Improved antifilarial activity of ivermectin in chitosan–alginate nanoparticles against human lymphatic filarial parasite *Brugia malayi. Parasitol. Res.,* **112**: 2933-2943. https://doi.org/10.1007/s00436-013-3466-4

Altmeyer, C., Karam, T.K., Khalil, N.M. and Mainardes, RM., 2016. Tamoxifen-loaded poly (L-lactide) nanoparticles development, characterization and in vitro evaluation of cytotoxicity. *Mater. Sci. Eng.,* **60**: 135-142. https://doi.org/10.1016/j.msec.2015.11.019

Basu, S., Mukherjee, B., Chowdhury, S.R., Paul, P., Choudhury, R., Kumar, A., Mondal, L., Hossain,

C.M. and Maji, R., 2012. Colloidal gold-loaded, biodegradable, polymer-based stavudine nanoparticle uptake by macrophages in vitro study. *Int. J. Nanomed.,* **7**: 6049. https://doi.org/10.2147/IJN.S38013

Day, C.M., Hickey, S.M., Song, Y., Plush, S.E., Garg, S. and Nove, 2020. Novel tamoxifen nanoformulations for improving breast cancer treatment old wine in new bottles. *Molecule*, **25**: 1182. https://doi.org/10.3390/molecules25051182

Dhawan, A., Mahima, B. and Devendra, P., 2009. Comet assay a reliable tool for the assessment of DNA damage in different models. *Cell Biol. Toxicol.,* **25**: 5-32. https://doi.org/10.1007/s10565-008-9072-z

Diao, H., Cheng, N., Zhao, Y., Xu, H., Dong, H., Thamm, D.H., Zhang, D. and Lin, D., 2019. Ivermectin inhibits canine mammary tumor growth by regulating cell cycle progression and WNT signaling. *BMC Vet. Res.,* **15:** 1-10. https://doi.org/10.1186/s12917-019-2026-2

Divya, K. and Jisha, M.J.E.C., 2018. Chitosan nanoparticles preparation and applications. *Environ. Chem. Lett.,* **16**: 101-112. https://doi.org/10.1007/s10311-017-0670-y

Dou, Q., Chen, HN., Wang, K., Yuan, K., Lei, Y., Li, K., Lan, J., Chen, Y., Huang, Z., Xie, N. and Zhang, L., 2016. Ivermectin induces cytostatic autophagy by blocking the PAK1/Akt Axis in breast cancer ivermectin induces cytostatic autophagy. *Cancer Res.,* **76:** 4457-4469. https://doi.org/10.1158/0008-5472.CAN-15-2887

Ghanbarzadeh, S., Hariri, R., Kouhsoltani, M., Shokri, J., Javadzadeh, Y. and Hamishehkar, H., 2015. Enhanced stability and dermal delivery of hydroquinone using solid lipid nanoparticles. *Colloids Surf. B.,* **136**: 1004-1010. https://doi.org/10.1016/j.colsurfb.2015.10.041

Guo, D., Dou, D., Li, X., Zhang, Q., Bhutto, Z.A. and Wang, L., 2018. Ivermection-loaded solid lipid nanoparticles: preparation, characterisation, stability and transdermal behaviour. *Artif. Cells Nanomed. Biotechnol.,* **46:** 255-262. https://doi.org/10.1080/21691401.2017.1307207

Harivardhan, R.L., Vivek, K., Bakshi, N. and Murthy, R.S., 2006. Tamoxifen citrate loaded solid lipid nanoparticles (SLN™): preparation, characterization, *in vitro* drug release, and pharmacokinetic evaluation. *Pharm. Dev. Technol.,* **11**: 167-177. https://doi.org/10.1080/10837450600561265

Honary, S. and Zahir, F.J.T.J.P.R., 2013. Effect of zeta potential on the properties of nano-drug delivery systems-a review part 1. *Trop. J. Pharm. Res.,* **12:** 255-264. https://doi.org/10.4314/tjpr.v12i2.19

Laing, R., Gillan, V. and Devaney E., 2017. Devaney ivermectin–old drug, new tricks? *Trends Parasitol*., **33:** 463-472. https://doi.org/10.1016/j.pt.2017.02.004

Mailk, A.A., Wani, K.A. and Ahmad, S.R.J.J.S., 2012. Breast conservative therapy. *J. Breast Cancer*, **15:** 7-14. https://doi.org/10.33883/jms.v15i1.103

Maji, R., Dey, N.S., Satapathy, B.S., Mukherjee, B. and Mondal, S., 2014. Preparation and characterization of Tamoxifen citrate loaded nanoparticles for breast cancer therapy. *Int. J. Nanomed.,* **9**: 3107-3108. https://doi.org/10.2147/IJN.S63535

Meißner, T., Potthoff, A. and Richter, V., 2009. Suspension characterization as important key for toxicological investigations. *J. Phys. Conf. IOP Publ.,* **170**: 12012. https://doi.org/10.1088/1742-6596/170/1/012012

Mitri, K., Shegokar, R., Gohla, S., Anselmi, C. and Müller, R.H., 2011. Lipid nanocarriers for dermal delivery of lutein: preparation, characterization, stability and performance. *Int. J. Pharm.,* **414**: 267-275. https://doi.org/10.1016/j.ijpharm.2011.05.008

Moin, A., Wani, S.U., Osmani, R.A., Abu Lila, A.S., Khafagy, E.S., Arab, H.H., Gangadharappa, H.V. V., Allam, A.N., 2021. Formulation, characterization, and cellular toxicity assessment of tamoxifen-loaded silk fibroin nanoparticles in breast cancer. *Drug Delivery,* **28**: 1626-1636. https://doi.org/10.1080/10717544.2021.1958106

Molinari, G., Soloneski, S., Reigosa, M.A. and Larramendy, M.L., 2009. *In vitro* genotoxic and cytotoxic effects of ivermectin and its formulation ivomec® on Chinese hamster ovary (CHOK1) cells. *J. Hazard. Mater.,* **1-3**: 1074-1082. https://doi.org/10.1016/j.jhazmat.2008.10.083

Mukherjee, B., Santra, K., Pattnaik, G. and Ghosh, S., 2008. Preparation, characterization and *in-vitro* evaluation of sustained release protein-loaded nanoparticles based on biodegradable polymers. *Int. J. Nanomed.,* **3**: 487. https://doi.org/10.2147/IJN.S3938

Mukherjee, B., Santra, K., Pattnaik, G. and Ghosh, S., 2008. Preparation, characterization and *in-vitro* evaluation of sustained release protein-loaded nanoparticles based on biodegradable polymers. *Int. J. Nanomed.,* **3:** 487. https://doi.org/10.2147/IJN.S3938

Nokhodi, F., Nekoei, M. and Goodarzi, M.T.J.J.M.S.M.M., 2022. Hyaluronic acid-coated chitosan nanoparticles as targeted-carrier

of tamoxifen against MCF7 and TMX-resistant MCF7 cells. *J. Mater. Sci.,* **33**: 1-14. https://doi.org/10.1007/s10856-022-06647-6

Rostami, S., Tafvizi, F. and Kheiri, M.H.R., 2022. Manjili, high efficacy of tamoxifen-loaded L-lysine coated magnetic iron oxide nanoparticles in cell cycle arrest and anti-cancer activity for breast cancer therapy. *Bioimpacts*, **12**: 301. https://doi.org/10.34172/bi.2021.23337

Sahana, B., Santra, K., Basu, S. and Mukherjee, B., 2010. Development of biodegradable polymer based tamoxifen citrate loaded nanoparticles and effect of some manufacturing process parameters on them a physicochemical and *in-vitro* evaluation. *Int. J. Nanomed.,* **5**: 621. https://doi.org/10.2147/IJN.S9962

Soliman, W.E., Khan, S., Rizvi, S.M., Moin, A., Elsewedy, H.S., Abulila, A.S. and Shehata, T.M., 2020. Therapeutic applications of biostable silver nanoparticles synthesized using peel extract of *Benincasa hispida*: Antibacterial and anticancer activities. *J. Nanomater.,* **10:** 1954. https://doi.org/10.3390/nano10101954

Tang, M., Hu, X., Wang, Y., Yao, X., Zhang, W., Yu, C., Cheng, F., Li, J. and Fang, Q., 2021. Ivermectin, a potential anticancer drug derived from an antiparasitic drug. *Pharma. Res.,* **163**: 105207. https://doi.org/10.1016/j.phrs.2020.105207

Vivek, R., Babu, V.N., Thangam, R., Subramanian, K.S. and Kannan, S., 2013. pH-responsive drug delivery of chitosan nanoparticles as tamoxifen carriers for effective anti-tumor activity in breast cancer cells. *Colloids Surf. B.,* **111**: 117-123. https://doi.org/10.1016/j.colsurfb.2013.05.018

Wozniak, K., Kolacinska, A., Blasinska-Morawiec, M., Morawiec-Bajda, A., Morawiec, Z., Zadrozny, M. and Blasiak, J., 2007. The DNA-damaging potential of tamoxifen in breast cancer and normal cells. *Arch. Toxicol.,* **81**: 519-527. https://doi.org/10.1007/s00204-007-0188-3

Zhan, X., and Li, N., 2021. *The anti-cancer effects of anti-parasite drug ivermectin in ovarian cancer, in ovarian cancer-updates in tumour biology and therapeutics*. IntechOpen. https://doi.org/10.5772/intechopen.95556

Zhang, H., Wang, C., Chen, B. and Wang, X., 2012. Daunorubicin-TiO2 nanocomposites as a “smart” pH-responsive drug delivery system. *Int. J. Nanomed.,* **7**: 235. https://doi.org/10.2147/IJN.S27722